The evolution of galaxy clustering since $z = 1.5$ in the ALHAMBRA survey

Pablo Arnalte-Mur[1], and The ALHAMBRA Team[1]

[1] Institute for Computational Cosmology, Department of Physics, Durham University, South Road, Durham DH1 3LE, United Kingdom

Abstract

The study of galaxy clustering at different redshifts is an important tool to obtain information about the process of growth of structures in the Universe, and about galaxy formation and evolution. We present the preliminary results of our measurements of the clustering of galaxies at different redshifts ranging from $z = 0.3$ to $z = 1.5$ using data from the ALHAMBRA Survey. This photometric survey has mapped a total area of $4 \, \mathrm{deg}^2$ using a total of 20 medium-band optical filters, and three broad-band NIR filters. It thus provides a deep sample ($I < 25$) with very accurate photometric redshift measurements ($\sigma_z \lesssim 1.3\%$). We measure the correlation function for different galaxy samples to study the evolution with redshift of the clustering properties of different galaxy populations selected by luminosity.

1 Introduction: the ALHAMBRA survey

The Advanced Large Homogeneous Area Medium-Band Redshift Astronomical (ALHAMBRA) Survey [7] is a pencil-beam, multi-band photometric survey with the aim of studying cosmic evolution over a large range in redshift. It covers a total of $4 \, \mathrm{deg}^2$ in 8 separated fields, using a photometric system designed to exploit the photometric redshift (photo-z) technique at maximum [5]. In this way it provides accurate photo-z estimates and spectral classification for the different objects and, at the same time, it samples a statistically significant volume at different redshifts. The survey has been carried out using the 3.5-m telescope at the Centro Astronómico Hispano-Alemán (CAHA)[2], using the Large Area Imager for Calar Alto (LAICA) for the optical observations, and Omega-2000 for the near-infrared (NIR).

---

[1] J. A. L. Aguerri, E. J. Alfaro, T. Aparicio-Villegas, N. Benítez, T. Broadhurst, J. Cabrera-Caño, F. J. Castander, J. Cepa, M. Cerviño, D. Cristóbal-Hornillos, A. Fernández-Soto, R. M. González Delgado, C. Husillos, L. Infante, I. Márquez, V. J. Martínez, J. Masegosa, M. Moles, A. Molino, A. Montero-Dorta, A. del Olmo, J. Perea, F. Prada, J. M. Quintana, M. Stefanon

[2] http://www.caha.es/

The optical filter system of the survey [1] consists of a set of 20 contiguous, equal-width, medium-band filters covering the full optical spectrum, between 3500 and 9700 Å. The width of each of these filters is $FWHM \simeq 310$ Å. This is complemented by the use of the standard NIR filters J, H, K_s. The expected depth of the survey varies between $m \simeq 25$ for the bluest filters to $K_s \simeq 23$ (all magnitudes are in the AB system).

Given the depth and un-biased selection function of the resulting galaxy catalogue, it allows for the study of the evolution of galaxy clustering over a large range in redshift. Given the geometry of the fields, this analysis is possible for small and intermediate scales ($r \lesssim 30\,h^{-1}\,\mathrm{Mpc}$). Galaxy clustering at these scales can provide important information about the relation between the galaxies and dark matter haloes hosting them.

In this talk, we briefly present the methods used to study the two-point correlation function of different samples of galaxies from the ALHAMBRA catalogue, and show preliminary results regarding the dependence of the clustering on redshift and galaxy luminosity. The main problem when doing this is the smearing of the galaxies' positions in the radial direction due to the use of photo-z. For this reason, we use the projection algorithm for recovering the real-space correlation function described in [2].

2 Data used

In this work, we use the data from the internal data release 4 (DR4) of the ALHAMBRA catalogue. This is a preliminary data release that provides PSF-corrected magnitudes and photo-z estimates for a catalogue of objects selected in the synthetic $F814W$ band (similar to I). The photo-z are estimated using the BPZ code [4], using an improved method for the photometric calibration. Comparison with the ~ 3000 available spectra in the surveyed fields gives a value of $\sigma_z = 0.0125(1 + z)$ for the dispersion of the photo-z values. Details of the catalogue will be presented in [8].

When doing clustering studies, it is important to characterise the angular selection function of the catalogue. In the case of ALHAMBRA, this is defined in first instance by the geometry of the fields. Each of them is formed by a total of 8 LAICA CCDs, arranged so that the surveyed area consists of two contiguous strips of $1° \times 0.25°$. We apply an additional mask based on the characteristics of the detection image (low exposure time near the borders, saturated pixels) and the location of bright stars. This mask reduces the effective area of the survey by $\sim 18\%$. Figure 1 shows this combined selection function for one of the fields. The DR4 catalogue used here contains data for 43 CCDs (out of the total of 64) in 7 ALHAMBRA fields. The effective area used is thus $A_{eff} = 2.21\,\mathrm{deg}^2$.

The photometric depth of the catalogue is $m_{F814W} \simeq 25$. However, to ensure that we have reliable photo-z estimates for the objects in the samples used, we perform the additional cut $m_{F814W} < 24$ to select our sample. We also remove stars from our sample using a combination of geometric and colour criteria [8]. The final catalogue used for our clustering calculation contains 149794 galaxies, and the median redshift of the sample is $z_{med} = 0.79$.
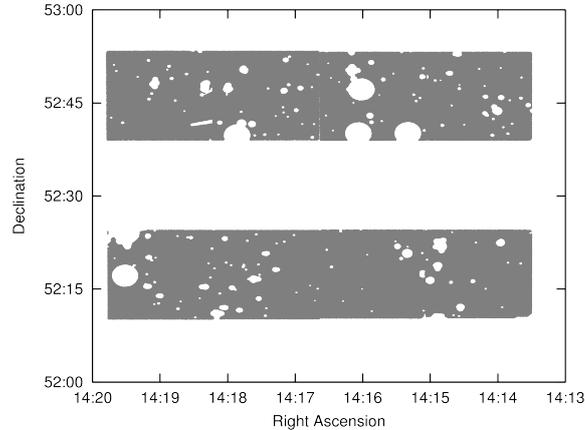
Figure 1:   Angular mask for the ALHAMBRA field 6. The shaded area corresponds to the regions fo the survey that are included in the calculations. This shows the particular geometry of the fields (defined by two contiguous pointings of the LAICA camera), and the effect of removing regions around bright stars or defects in the detection image.

3   Clustering results: luminosity segregation and evolution

In order to be able to study the dependence of the clustering properties on both luminosity and cosmic time, we build a series of subsamples from our catalogue, by making a selection in redshift and absolute magnitude. We select subsamples in three non-overlapping bins in redshift in the range $z \in [0.3, 1.5]$. We also apply a set of cuts in B-band absolute magnitude, M_B. We use 'threshold samples', meaning that we impose a faint luminosity threshold, but not a bright limit. The actual limits in M_B are defined following the evolution of the luminosity function characteristic luminosity $L^\star$. In this way, we follow the evolution with redshift of galaxy populations with an approximately constant ratio $L^{\mathrm{med}}/L^\star$, where L^{med} is the median luminosity of the sample. We show in Fig. 2 the actual cuts made in the redshift – absolute magnitude plane to define our samples.

In order to study the real-space clustering of the samples, avoiding the smearing effect due to the use of photo-z, we use the projected correlation function $w(r_p)$. This statistic is defined from the two-dimensional correlation function $\xi(r_p, \pi)$ as

$$w(r_p) = 2 \int_0^{\pi_{\mathrm{max}}} \xi(r_p, \pi) \mathrm{d}\pi \,, \tag{1}$$

where π denotes separations along the line-of-sight, and r_p separations perpendicular to it. The fact that w depends only on the transverse separation r_p, while the radial coordinate π is integrated over, means that it depends, at first order, only on the real-space clustering, as r_p is not affected by the redshift measurements. In the case of photo-z, the optimal value of the integration limit π_{max} depends of the typical redshift error of the sample σ_z, and is usually much larger than in the case of spectroscopic samples. In our calculations, we use values in the range $\pi_{\mathrm{max}} = 100 - 200 \, h^{-1} \, \mathrm{Mpc}$, depending on the sample. For details of this
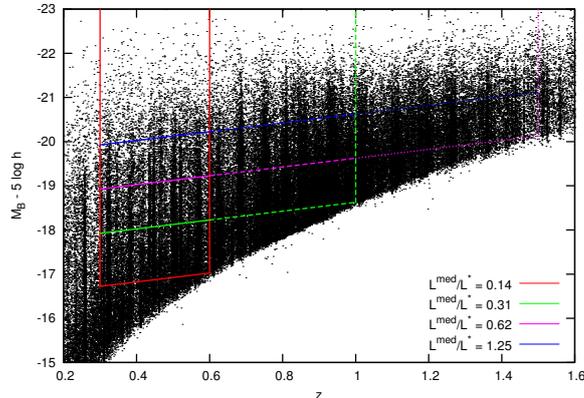
Figure 2: Absolute B-band magnitude vs. redshift z for the catalogue used. The different lines show the boundaries of the samples we select for our analysis. The cuts in luminosity are defined following the evolution of $L^{\star}$, so that the resulting $L^{med}/L^{\star}$ of each sample is approximately constant over the three redshift bins.

method, see [2]. We estimate the error in our measurements by using a bootstrap technique that makes use of the independence of the 8 surveyed fields.

We show in Fig. 3 our preliminary results for the projected correlation functions of each of our samples in the range $r_p \in [0.05, 30]\, h^{-1}\, \mathrm{Mpc}$. As expected, we obtain a clear luminosity segregation of the samples: in the three redshift bins, the clustering signal is stronger for more luminous samples. The $w(r_p)$ for the different samples follow approximately a power law, except for the largest scales considered, where we see a more pronounced decline. This is a result of the integral constraint, an observational effect due to the finite size of the sample which affect the correlation function at scales of the order of the field size. In the case of the projected correlation function, the amplitude of this effect depends also on the value of $\pi_{\max}$ used in the integration of equation (1). When we fit the obtained $w(r_p)$, we account for the effect of the integral constraint in the models.

In order to study the change of the clustering properties with luminosity and redshift, we fit the obtained projected correlation function $w(r_p)$ of each sample to a power law model in the range $r_p \in [0.2, 30]\, h^{-1}\, \mathrm{Mpc}$. We use the fact that a power law model for $w(r_p)$ corresponds also to a power law model for the real-space correlation function $\xi(r) = \left(\frac{r}{r_0}\right)^{\gamma}$, and quote our results as constraints on the correlation length r_0 and the slope γ, as it is usually done. We show the dependence of these fitted parameters on luminosity and redshift in Fig. 4. We see clearly the effect of luminosity segregation for the three bins in redshift. We also see the effect of the evolution of clustering with redshift, specially between the two redshift bins around $z \sim 1$.
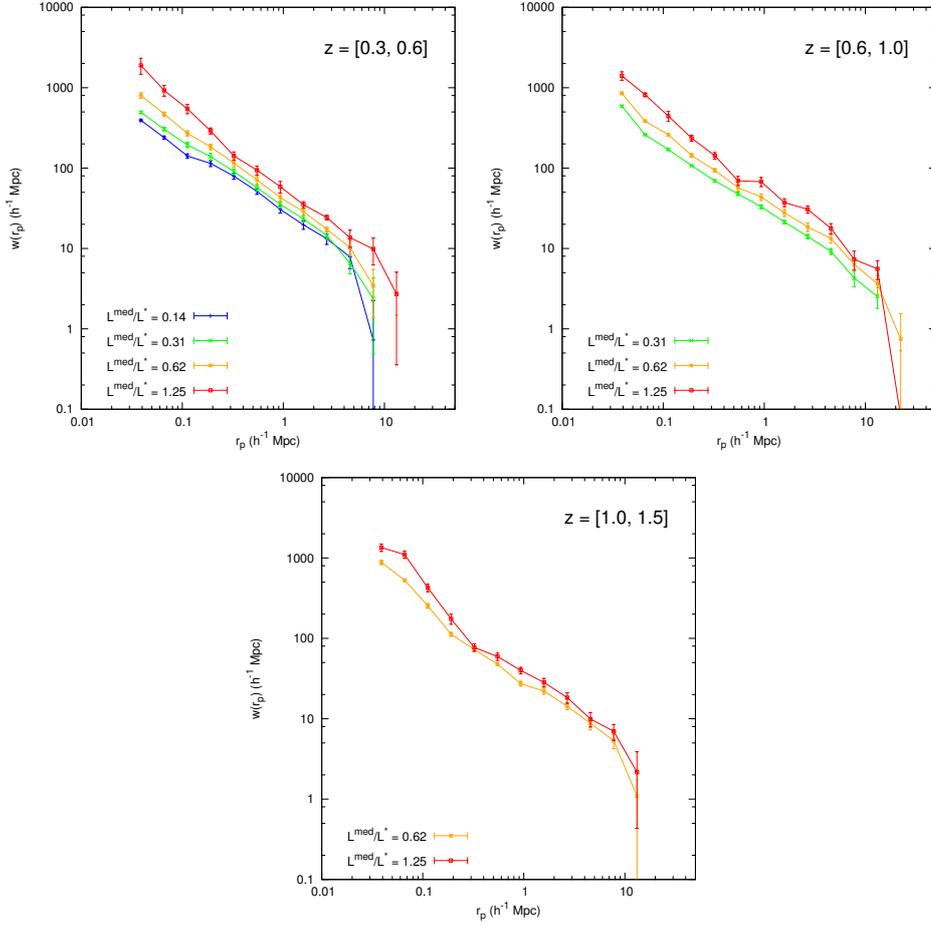
Figure 3: The projected correlation functions $w(r_p)$ obtained for the different samples selected by luminosity in the three redshift bins considered.
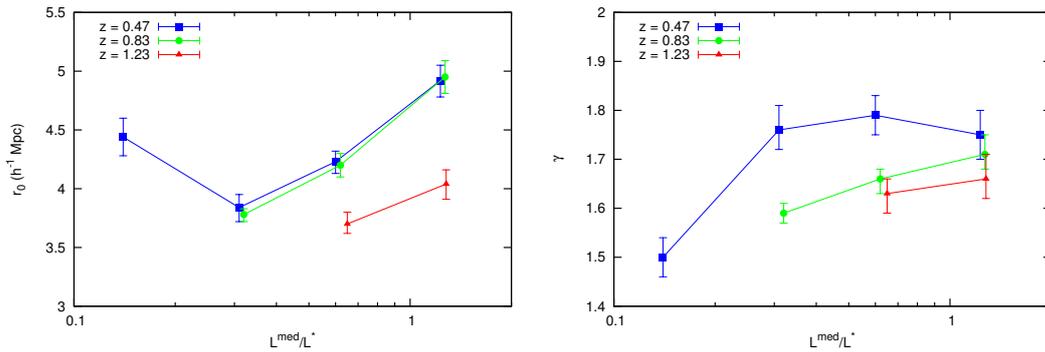
Figure 4: Parameters r_0 (left) and γ (right) obtained from the power-law fits for the different samples, as function of the median luminosity L^{med} of the samples, for each of the redshift bins.

4   Discussion and future work

In this talk, we have shown how we can use the photometric redshift catalogue from the AL-HAMBRA survey to study real-space clustering through the use of the projected correlation function $w(r_p)$. We have also shown the results obtained using a preliminary data release, and a preliminary analysis of the luminosity segregation and its evolution, in a qualitative way.

We plan to extend this work in different ways. On one side, we will perform an extensive study of the reliability of our measurements, taking into account possible systematic effects, such as the modelling of both the angular and radial selection functions, differences in the line-of-sight integration limit π_{max}, or the error estimation method. To this end, we will use a set of mock catalogues produced using the method described in [6]. On the other side, we will perform a more detailed analysis of the results, using Halo Occupation Distribution (HOD) models to extract the halo properties corresponding to each galaxy population. We will also study the dependence of clustering on galaxy properties other than luminosity, such as colour or spectral type. This work will be presented in [3].

Acknowledgments

References

[1] Aparicio-Villegas, T., et al. 2010, AJ, 139, 1242

[2] Arnalte-Mur, P., Fernández-Soto, A., Martínez, V.J., et al. 2009, MNRAS, 394, 1631

[3] Arnalte-Mur, P., et al. 2012, in prep.

[4] Benítez, N. 2000, ApJ, 536, 571

[5] Benítez, N., et al. 2009, ApJ, 692, L5

[6] Merson, A. I., et al. 2013, MNRAS, 429, 556

[7] Moles, M., et al. 2008, AJ, 136, 1325

[8] Molino, A., et al. 2012, in prep.